WPJET2-CPR(18) 18745

C Makepeace et al.

The effect of Beryllium Oxide on retention in JET ITER-like wall tiles.

Preprint of Paper to be submitted for publication in Proceeding of 23rd International Conference on Plasma Surface Interactions in Controlled Fusion Devices (PSI-23)

This work has been carried out within the framework of the EUROfusion Consortium and has received funding from the Euratom research and training programme 2014-2018 under grant agreement No 633053. The views and opinions expressed herein do not necessarily reflect those of the European Commission.

The effect of Beryllium Oxide on retention in JET ITER-like wall tiles.

C. Makepeace[a], C. Pardanaud[b], M. Kumar[b], C. Martin[b], Y. Ferro[b], E. Hodille[b], P. Roubin[b], I. Borodkina[c,d], T.Dittmar[d], C.Ayres[e], P.Coad[e], A.Baron-Wiechec[e] I. Jepu[f], K.Heinola[g], A.Widdowson[e], S.Lozano-Perez[a] , and JET Contributors*

EUROfusion Consortium, JET, Culham Science Centre, Abingdon, OX14 3DB, UK
[a] Department of Materials, University of Oxford, Parks Road, Oxford OX1 3PH, UK
[b] Aix-Marseille Universite, CNRS, PIIM UMR 7345, 13397, Marseille, France
[c] National Research Nuclear University MEPHI, Moscow, 115409, Kashirskoe sh. 31, Russia
[d] Forschungszentrum Julich GMbH, Wilhelm-Johnen-Strasse, 52428 Julich, Germany
[e] CCFE, Culham Science Centre, Abingdon, OX14 3DB, UK
[f]National Institute for Laser Plasma and Radiation Physics, Bucharest-Magurele 077125, Romania
[g] University of Helsinki, PO Box 64, FI-00560 Helsinki, Finland
*See the author list of "X. Litaudon *et al* 2017 *Nucl. Fusion* 57 102001″

carmen.makepeace@materials.ox.ac.uk

Abstract:
This work is a preliminary publication investigating the microstructure, bonding and effect of beryllium oxide formation on retention in the JET ITER-like wall beryllium tiles. The tiles have been investigated by many techniques: Scanning Electron Microscopy (SEM) equipped with Energy Dispersive X-ray (EDX), Transmission Electron microscopy (TEM) equipped with both EDX and Electron Energy Loss Spectroscopy (EELs), alongside Raman Spectroscopy and Thermal Desorption Spectroscopy. This paper focuses on results seen in melted materials of the dump plate tiles in JET (positioned at the top of the reactor). From both our results and the literature, it is concluded that beryllium has formed micron deep oxide islands as opposed to the nanometric scales predicted under vacuum conditions. The deepest oxides analyzed were up to 2-micron thicknesses. The beryllium Deuteroxide (BeO_xD_y) bond was found with the use of Raman Spectroscopy. Further application of EELs, confirmed the presence of the oxides and an ongoing investigation into their structure. From the literature it is suggested that these oxides form at temperatures greater than 700K. At such temperatures beryllium diffusion through an oxide layer can occur, enabling further oxidation post earlier passivation at lower temperatures. Continual cyclic heating in the presence of oxygen from the plasma (even under UHV conditions) is expected to result in the oxides seen experimentally in this melt region. This retention mechanism is not considered to contribute dramatically to overall retention in JET, due to low levels of melt formation overall. However, this mechanism is thought the result of operation environment and melt formation. As a result, it could be of wider concern to ITER, dependent on ITER's operational conditions and wall temperatures.

Introduction:
Beryllium is the material of choice for the International Thermonuclear Experimental reactor (ITER) and as such is the subject of much research surrounding fuel retention due to the requirements of ITER's safety case. Tritium, a radioactive isotope of hydrogen and one of two hydrogen isotopes used in the fusion reaction, has an operational safety limit of 700g within the reactor vessel. The beryllium wall area alone, will equate to almost ~700m^2. Beryllium was chosen as the first wall cladding material due to: reduced chemical erosion (compared to previous carbon counterparts); a high melting point; a low Z number; and good oxygen gettering from the plasma.
The Joint European Torus (JET) moved to an ITER-like wall with beryllium limiters and a tungsten divertor in late 2010 and saw a factor of 20 reduction of retained hydrogen isotopes compared to a carbon wall. Since then three ITER-like wall campaigns have occurred producing reactor relevant materials for post mortem analysis. This paper focuses on work from the first campaign and beryllium materials originating from the apex of the reactor. This is an area where comparably larger volumes of melted material are produced in JET. Melted material appears to increase the propensity of beryllium oxidation, due to increased diffusion of beryllium to the surface, whereby oxygen from the plasma can react once more [1]. Despite beryllium's often touted claim of 'good oxygen gettering', the result of oxidation on retention is widely discussed [2]. Data from controlled lab experiments leads to a complicated understanding of hydrogen retention and oxidation. The results are briefly summarized below:
Early reports from [3] found that both water and oxygen can independently oxidize beryllium to ~ 3 monolayer thick islands. If both H_2O and oxygen are present coincidently, further growth can occur to ~ 6 monolayer depths [4]. However, formation of OH bonds at the surface was not discovered. Retention was found to largely reduce when oxidized beryllium was exposed to hydrogen, compared to clean beryllium [5]. Desorption of H was found at 320K for BeO surface and 450K for the clean surface. Zalkind promoted oxide islands formation

by nucleation at critical oxygen coverages above 2-3 monolayers, followed by lateral growth. Ion implantation was seen to double the oxygen sticking coefficient and increase the oxidation rate significantly [6]. Similarly, pre-adsorbed H significantly reduced the quantity of adsorbed oxygen on the surface. At T>700K the oxygen nucleates without chemisorption. Thermal desorption data, above all must be considered carefully [7]. The ease at which beryllium can oxidize, even under ultra-high vacuum conditions, has led authors to suggest samples were free of oxidation, when more likely partial oxide layers had already formed [8].

Experimental Method:

Tiles taken from the first ITER-like wall campaign (2011-2012) were cut into individual castellations as previously described in [9] to avoid sample heating and produce thermal desorption relevant samples (1cm^2 x 250mm). Dump plate tiles orientated at the top of the vessel are indicated in Figure 1; including the 2B2C dump plate tile photo (right) showing surface melting along the central ridge. For comparison, limiter tiles 2XR10 and 4D14 from the mid plane of the inner and outer walls respectively are also indicated in the Figure 1 poloidal cross section of JET. SEM and EDX (Tescan) were used to analyse the surface chemistry of tiles; using 5, 10 and 20kV accelerating voltages. The Casino software [10] was applied to provide a rough estimate of the corresponding interaction volumes from which the characteristic X-Rays are produced, and therefore an estimate of the depth of the oxides present. Further image analysis was undertaken using Image-J to gain an estimate of the average oxide island size and distribution [11]. Raman Spectroscopy was untaken on both the limiter and dump plate tiles in back-scattering geometry, using a Horiba-Jobin Yvon LabRAM apparatus (x100 objective, 0.9 numerical aperture, laser wavelength of 514.4nm and laser power of ~1mWμm^{-2}). The Raman Map discussed in this report was taken with a lateral resolution of 500nm and focused on one area in particular, which lead to the discovery of the Be-OD bond. Further information can be found in the publication by Kumar et al [15]. Transmission electron microscopy lamella of a cross section through the Raman mapped area (and other areas additionally) were prepared via Focused Ion Beam (FIB). A dual beam FEI Helios (FIB) was used for this purpose. The preparation route was standard to beryllium materials, involving platinum deposition on the surface, first with the electron beam, followed by low current ion beam platinum deposition, until a protective layer of 2µm is present. A 30kV beam was used to trench around the area of interest, followed by undercutting. The beam current was 22nA and 9nA respectively. Lastly the area is lifted out and attached to a semi-circular omni probe copper mount, where the sample can then be thinned to ~100nm and further low energy cleaning can occur to take the sample to sub 100nm thicknesses. Samples were transferred to the Jeol-ARM200f transmission electron microscopy complete with standard TEM, Scanning TEM, EDX and EELs detectors. STEM was used predominantly and in conjunction with EDX and EELs. Due to the limitations of EDX in detecting beryllium, EELs can be used to good effect to understand the exact stoichiometry's present between Be and O, with future work continuing to investigate the presence of H isotopes in the low loss region of the spectra. Thermal desorption data were collected on samples from similar locations along the tiles and the first results shown. The process involves back heating a sample under a 10°C/min thermal ramp under vacuum. The gaseous species desorbed from the surface are then measured via quadrupole mass spectrometer. Further work is ongoing to model TDS data with the Tritium Migration Analysis Program (TMAP7) and will be the subject of future publication.

Figure 1: Image of a) poloidal cross section of JET, showing the position of the 2B2C dump plate tile, and b) the 2B2C tile with melted central ridge.

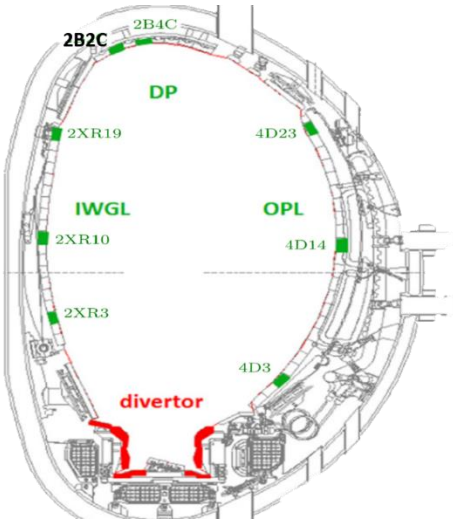

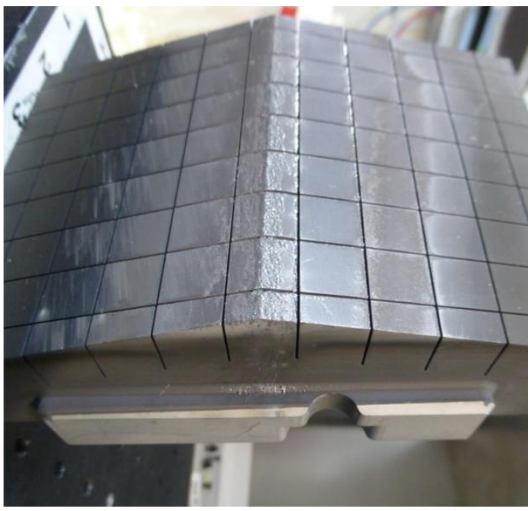

Experimental Results and Discussion:

Initial scanning electron microscopy studies of the melted sample surface were undertaken, to gain insight into the average surface oxide coverage. EDX used at 3 different accelerating voltages: 5, 10 and 20kV to estimate the extent of oxidation up to approximately 250nm, 400nm and 2000nm respectively; showed the oxides to be present and consistent from the surface to the maximum depth in the melted material. A comparison at the maximum depth of 2µm is given in the table below. Limiter tiles 2XR10 and 4D14 are given for completeness.

	20kV ~2µm depth		
Position in JET	number of particles	average particle size	Percentage Area
outer poloidal limiter eroded	1127	0.172um	0.975
outer poloidal limiter deposited	14977	8.604um	17.965
inner poloidal limiter eroded	12298	0.117um	7.196
inner poloidal limiter deposited	10680	0.160um	7.496
dump plate melted material	3804	6.298um	19.894

Table 1: Comparison of oxidation levels between limiter tiles and melted dump plate tile.

The results show that the average particle size of 2µm depth oxide particles is much greater on the surface of beryllium materials exposed to higher temperatures and melt events, excluding layers built up by codeposition on the regions governed by deposition in the limiter tiles. It will be show by EELs subsequently that these deposits have a very different structure to the metallic oxidation occurring during, or as the result of heating and melt behaviour. It is therefore more difficult using this method to determine the extent of oxidation in co-deposited tiles when the deposit extends beyond 2µm, and has a far reduced oxygen to beryllium ratio.
An in-depth analysis of a specific region of the melted castellation, first studied by Raman Spectroscopy follows. Figure 2 shows a region of melted material. This region is positioned at the left toroidal castellation gap and appears the result of erosion across the face of the castellation from right to left toroidally. This is consistent with the plasma direction. The area to the right of the melted ridge has a micron sized crack network connecting islands of eroded material. Larger macro-scale cracks are seen along all edges of the castellation, bridging regions of melted material (heaps) to the lower eroded zones. Cracking is likely a response to the large thermal shocks the dump plate castellations have received during operation. Presence of oxidation and the differences between the oxide's thermal expansion and S65C beryllium will increase the level of stress present in the material as well. These eroded areas have been studied microstructurally and are an area of ongoing investigation. Unfortunately, marker layers produced on these tiles complicate material chemistry due to mixing at high temperatures. Nevertheless, the oxides formed are free of nickel contaminants. Samples without nickel impurities will subsequently be analysed to understand the effect of impurities on oxidation kinetics.

Figure 2: a) SEM secondary electron image of melted ridge (left toroidal edge of the castellation), and b) the analysis region at higher magnification (0.8 kx), and c) Raman schematic of the region after analysis, showing surface chemistry contributions spatially. The red box indicates the area of the TEM

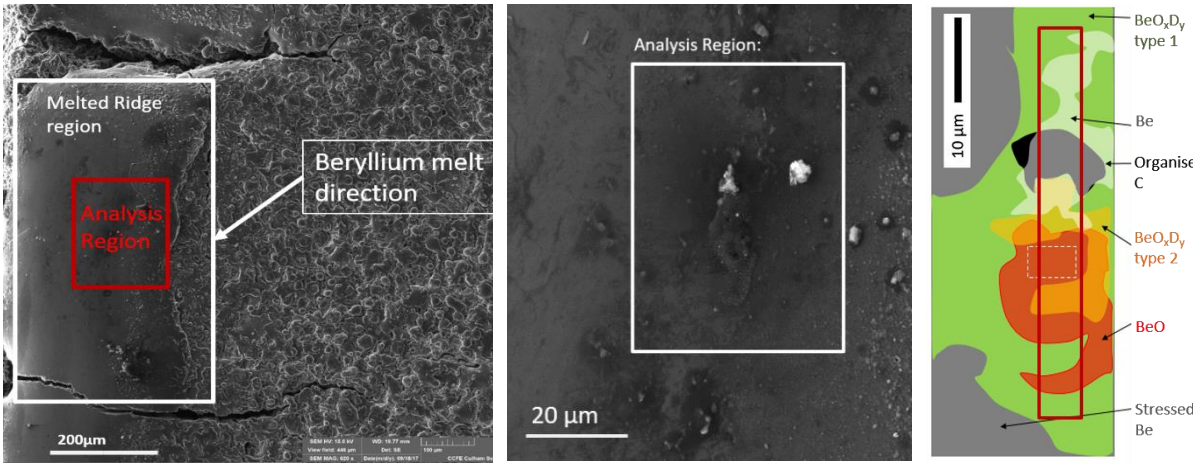

(a) (b) (c)

Raman analysis of this region showed for the first time, the presence of the BeO_xD_y bond confirmed by comparison to Infra-Red studies of HOBeOH, HBeOH and HBeOBeH, found in the literature [12]. Further calculations using both DFT and BeO samples have confirmed the wurtzite structure, however the exact stoichiometry of the BeOD bond is yet to be confirmed. For further analysis of the Raman technique please see the publication by Kumar et al [15]. What can be seen from the Raman schematic in Figure 2, is the complex nature of the surface chemistry present without exception in all JET tiles. Analysis of the Raman spectra eluded to the presence of multiple forms (3) of the Be-OD bond with varying stoichiometries. As a result, a Transmission Electron Microscopy (TEM) lamella of the region was produced. The area of the lift-out taken is shown in Figure 2c by the red box outlined.

Figure 3: Top) Scanning Transmission Electron Micrograph (stitched together as an overview of sample), bottom: a) STEM image showing region of EDX maps, b) background subtracted EDX map of Oxygen, showing a section of the beryllium oxide area on the lift-out.

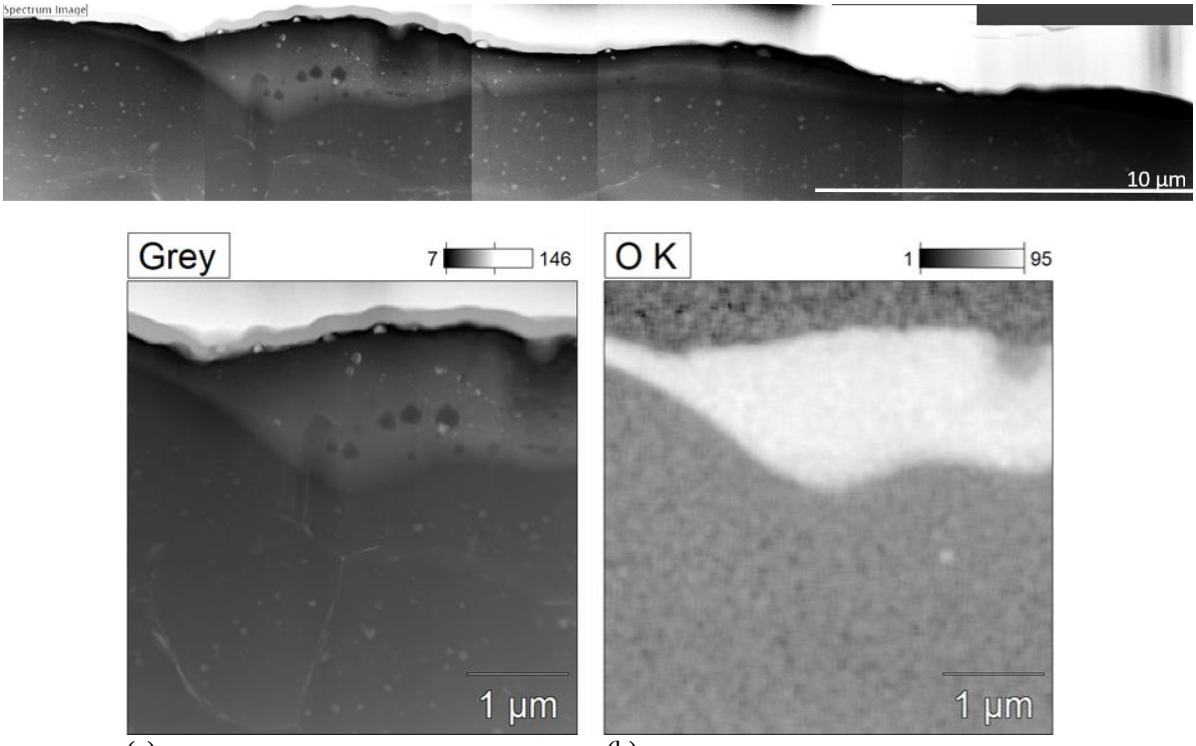

(a) (b)

Figure 3 shows the extent of oxidation in the Raman analysis region, spanning ~20µm laterally, and at greatest depth ~2µm. The EDX of the sample shows a clear oxidation boundary however in-depth EELs of the region shows oxidation variability independent of grain orientation.

Figure 4: a) A map of beryllium analysed via EELs showing the atomic percentage of beryllium present. b) the corresponding map of O in atomic percent

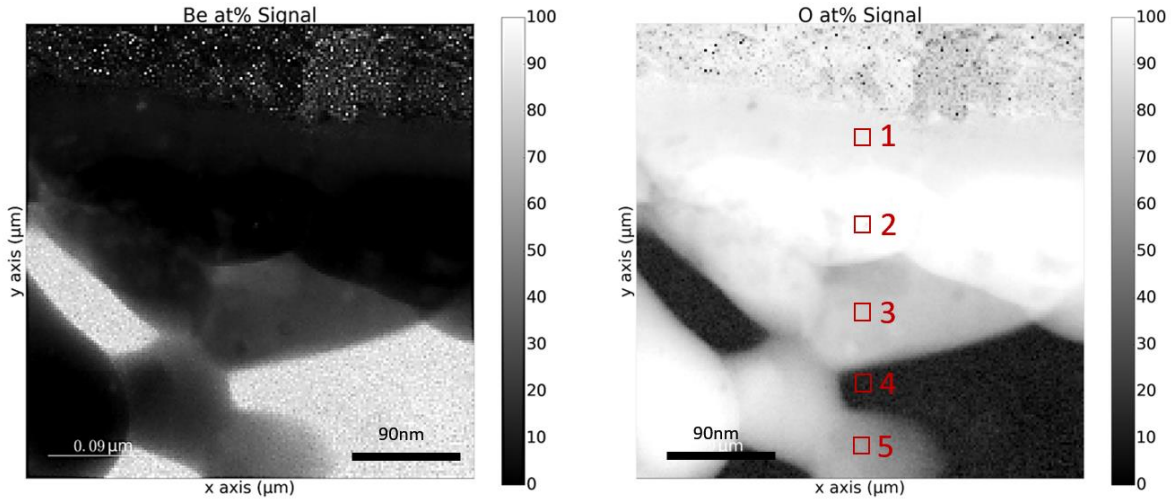

(a) (b)

Point in EELs Oxygen at% map	Beryllium atomic %	Oxygen atomic %
1	7.6	92.4
2	0	100
3	27.4	72.6
4	81.5	18.5
5	42.9	57.1

Table 2: List of beryllium and oxygen stoichiometries at oxidized points listed in Figure 4.

Figure 5: EELs spectra extracted from Figure 4 showing the fine structure a) of the beryllium ~113eV edge appearing in less oxidised grains and b) of the oxide edge at ~540eV

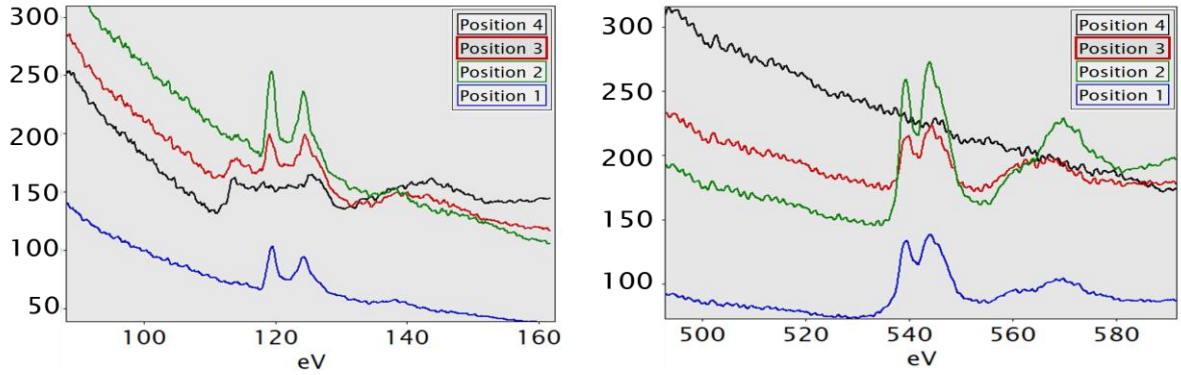

Figure 6: (a) the region of the inner wall limiter deposit mapped with EELs in STEM mode, (b) the corresponding O atomic percentage map, and c) the corresponding Be atomic percentage map.

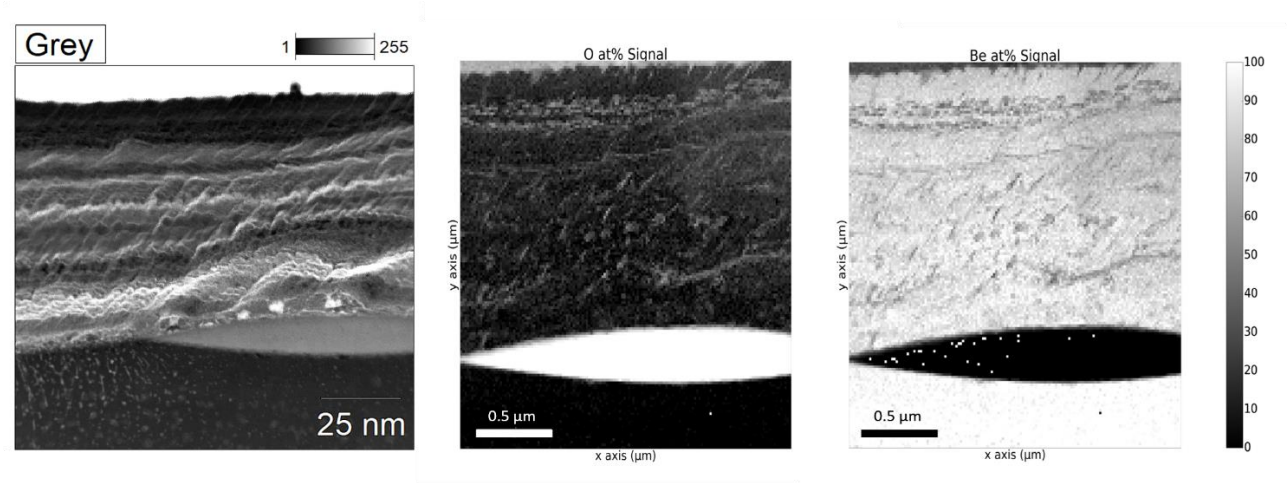

(a) (b) (c)

Figure 4 shows the extent of oxidation present in the first 400-500nm of the melted samples' surface. The grains are clearly oxidized to different extents with 3 grains clearly seen as almost pure beryllium in Figure 4a (white) and correspondingly black in Figure 4b. Interestingly the extent of oxidation does not appear to be related to the grain depth nor the grain orientation. As such ongoing work modelling the fine structure of the EELs spectra, is occurring to determine whether contributions from H isotopes appear in the spectra and whether these can be analysed consistently. The extracted spectra seen in Figure 5, show that subtle changes are in fact occurring in the fine structure. The 570eV EELs edge maxima is shifting position relative to the oxidation in the grain, whilst the intensity is changing in the 537 and 543 eV peaks. Most interestingly of all is the behaviour of the beryllium fine structure. At higher oxidation, the 113eV edge is missing. Instead, under oxidation 2 new peaks at 120 and 125eV appear with intensity varying with oxidation levels. Finally, analysis of the zero-loss region is perhaps of most interest. Additionally, to metallic plasmons is the presence of the low loss spectra. If hydrogen isotopes can be linked to the EELs spectra they will be seen here. Early work shows large edges appearing at 20eV, however

further work is needed to determine whether this is the result of deuterium or an oxide plasmon. Modelling of these results is ongoing.
Comparatively results from deposit formed on the inner wall limiter deposition zone (the shadowed wing region) show approximately 2µm of deposit formed above the surface of a surface oxide. These 2 phase regions clearly show the differences in oxidation found between metallic oxidation at the surface, and surface co-deposition. Figure 7 shows the fine edge structures extracted from position 7 (the deposit), position 8 (the crystalline oxide) and position 9 the original beryllium surface (metallic beryllium). It is clear to see that the fine structure of the oxide edge is significantly changed between deposits containing 20-35at% O and crystalline BeO oxidized at the surface. The 2 oxide edges at ~539 and 545eV are much broader and less intense, whilst the broader peak at ~570eV is not visible. Similarly the beryllium fine structure retains greater likeness with bulk beryllium in the deposit region than an oxide maintaining the 113eV edge, with almost no further intensity increase across its energy span.

Figure 7: EELs spectra extracted from Figure 5 showing the fine structure a) of the beryllium 113eV edge appearing in the deposited, oxide and beryllium bulk phases b) of the oxide edge appearing in the deposited, oxide and beryllium bulk phase

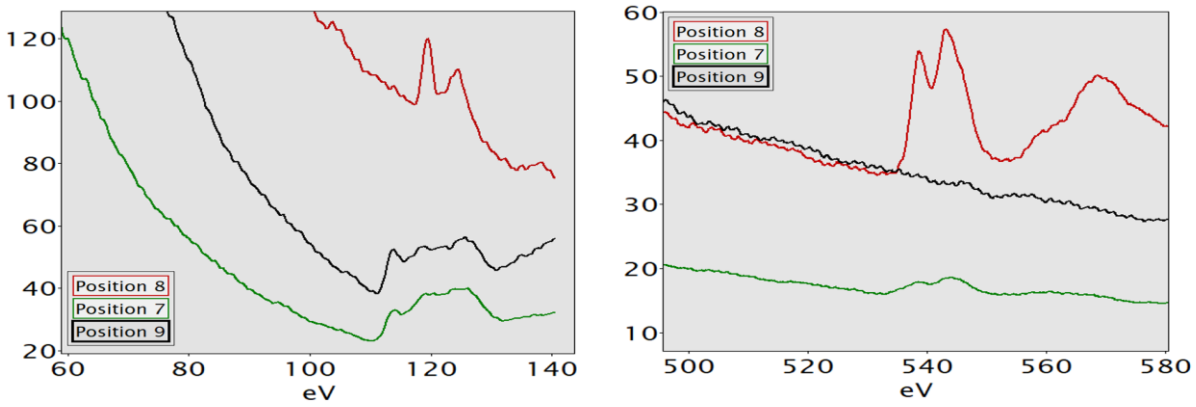

What can be seen comparatively between the melted region's EELs maps and those of the deposit is the relative percentage changes in oxidation. The melted region occurs with grains ranging from no oxidation, to 25%, 75% and 100% oxidation. The deposited region however shows an amorphous nature with ring patterns in the TEM under selected area diffraction. Additionally, the level of oxidation within the deposit is more uniform ranging from 20-35%. The deposited material appears to be much less ordered with at best nanometric scale horizontal regions of BeO far from stoichiometric ratios of 1:1. This has led to discussion of modelling such materials' thermal desorption.
Eroded central regions of the limiter tiles are the most ordered and simplest systems to model. Early work in the TEM has shown this. There is a low density of dislocations present in the material, almost no surface oxidation has occurred, and the 1-3µm grains appear largely uniform (Figure 8). Modelling of these materials via the Tritium Migration Analysis Program (TMAP7) is the most straight forward of the three microstructures presented (melted, eroded and deposited). Data from IBA are compiled to give a starting implanted distribution of Deuterium, with the main segment of the code being a beryllium block of half the thickness of the sample. Diffusion is enabled throughout the block structure and recombination limited release governs at the surface. Agreement between experimental data and the code has been successful, however on application of the same approach to the deposited material, almost no agreement stands between the desorption peak position and the modelled result. A similar experience has occurred with the oxidation seen in melted material. Early efforts to apply a surface binding energy to the oxide equivalent to that of the Be-OD bond energy has been attempted. However, whilst agreement has improved work is ongoing and will be the subject of another publication.
Currently the comparative raw data of desorption between an eroded region, a melted region and a deposited region of the 2010-2012 campaign are given for completeness (Figure 9). The melted region has comparably lower retention levels than those seen in both the eroded and deposited regions, which appears consistent with [16]. The deposited material remains the highest mechanism of retention. This is believed to be the result of the properties of the deposit and its microstructure. The sedimentary like structure which is highly porous (Figure 8a), could suggest that the desorption kinetics of the material have greatly changed. Physical processes such as surface area and molecular surface tension to pores may play a more fundamental role in the trapping behaviour of these materials. Further investigation of these traits with TMAP7 is planned and will be published in the future. From the raw data the desorption peak position of the melted material has shifted to higher temperatures of ~825K. Whilst the eroded material and melt material appear to have only one desorption peak, the deposited material shows earlier release at ~675K followed by a much larger release at 925K. It is also clear that desorption is not fully complete when reaching the maximum operating temperature of the TDS prior to beryllium evaporation.

Figure 8: a) Porous structure of the deposit, showing nanoscale voids potentially enabling D2 gas retention, b) TEM bright field image of eroded material, showing gas filled cavities along grain boundaries in crystalline metallic beryllium.

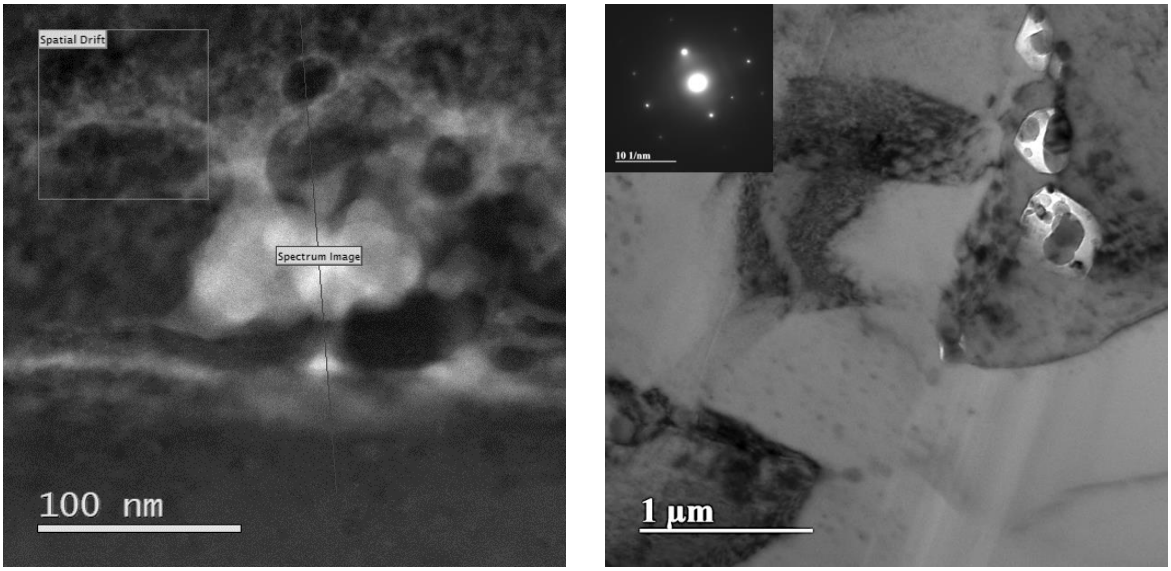

(a) (b)

Figure 9: Thermal Desorption data of an eroded, melted and deposited castellation.

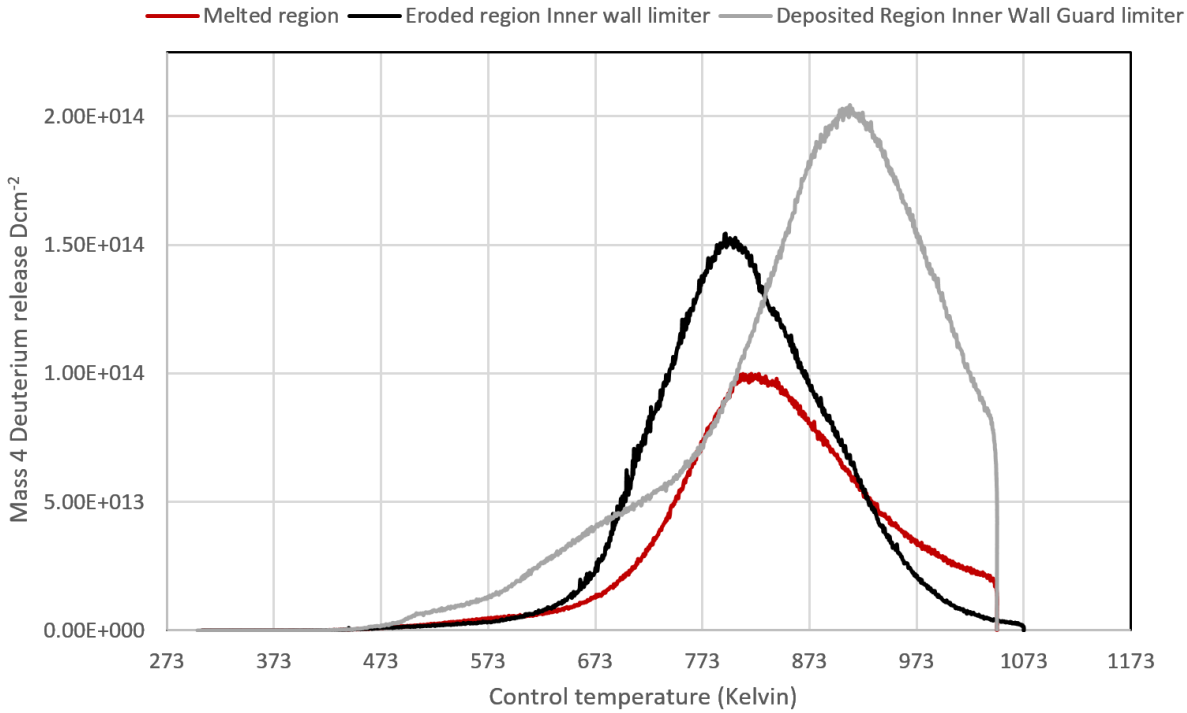

Conclusion:

The first early results of in depth EELs analysis following the discovery of the Be-OD bond with Raman have been reported. Ongoing modelling work, and EELs with standardised BeO materials is occurring to determine the influence of deuterium present in the EELs fine structure. Hydrogen isotopes are difficult to measure microscopically in the TEM. The benefits of 'seeing' hydrogen isotopes present spatially and at the microscale would be very useful in determining the mechanisms of retention.. The EELs results reflect those seen via Raman. Complex oxidation is present in the sample with 2 or more phases present. EELs unlike Raman is able to view the sub-surface structure beyond 50-100nm and portrays these behaviours present to micron depths. Early application of these microstructural findings to desorption data have started and continue. Application of a Be-OD bond

surface energy have started to be applied, whilst much greater investigation of the desorption differences between the deposit and eroded samples is needed. The results of desorption modelling will be the subject of future publication. Whilst the discovery of the Be-OD bond is interesting, retention behaviour connected to this bond appears limited in JET, simply due to low levels of melted material. In 2010-2011 (ILW1) ~19g of material is estimated to have occurred in the dump plate areas, 134g in 2012-2013 (ILW2), and ~30g in 2014-2015 (ILW3). As a result, it appears that retention in the first 0-3μm of such limited wall areas, is unlikely to be a significant contributor to the overall hydrogen retained in the whole of the reactor. Nevertheless, if operation conditions in ITER enable higher wall temperatures for longer periods in steady state, and additionally have greater ELMs and displacement events, oxide formation and the chemical retention seen here could be much more substantial. Additionally, it is clear in the raw TDS data that the presence of an oxide bond at the surface has led to higher desorption peak temperatures. From early modelling attempts with TMAP7 it is initially proposed that this could be due to a surface binding energy inhibiting desorption and release. Higher operating temperatures can additionally promote higher levels of H isotope diffusion into the bulk. Therefore, post dynamic out-gassing, a situation could exist under higher temperature operation, where an increase in diffusion is seen into the bulk, alongside a surface barrier being created. In both cases, a longer and higher temperature programmed desorption would need to take place to remove retained materials from the wall. This will most likely affect ITER baking operations.

"*This work has been carried out within the framework of the EUROfusion Consortium and has received funding from the Euratom research and training programme 2014-2018 under grant agreement No 633053. The views and opinions expressed herein do not necessarily reflect those of the European Commission*."

[1] D. W. Aylmore, S. J. Gregg, and W. B. Jepson, "The high temperature oxidation of beryllium. Part I. In dry oxygen," *J. Nucl. Mater.*, vol. 2, no. 2, pp. 169–175, 1960.

[2] A. Allouche, "Quantum modeling of hydrogen retention on partially oxidized beryllium," *J. Nucl. Mater.*, vol. 415, no. 1 SUPPL, pp. S721–S723, 2011.

[3] S. Zalkind, M. Polak, and N. Shamir, "Adsorption of hydrogen on clean and oxidized beryllium studied by direct recoil spectrometry," *Appl. Surf. Sci.*, vol. 115, no. 3, 1997.

[4] S. Zalkind, M. Polak, and N. Shamir, "The adsorption of H2O vs O2 on Beryllium," vol. 385, pp. 318–327, 1997.

[5] S. Zalkind, M. Polak, and N. Shamir, "Effects of preadsorbed hydrogen on the adsorption of O2, CO and H2O on beryllium," *Surf. Sci.*, vol. 539, no. 1–3, pp. 81–90, 2003.

[6] S. Zalkind, M. Polak, and N. Shamir, "Oxidation of ion-bombarded vs. annealed beryllium," *Surf. Sci.*, vol. 513, no. 3, pp. 501–510, 2002.

[7] A. Allouche, M. Oberkofler, M. Reinelt, and C. Linsmeier, "Quantum Modeling of Hydrogen Retention in Beryllium Bulk and Vacancies," *J. Phys. Chem. C*, vol. 114, no. 8, pp. 3588–3598, 2010.

[8] A. Allouche, "Quantum modeling of hydrogen retention on partially oxidized beryllium," *J. Nucl. Mater.*, vol. 415, no. 1 SUPPL, pp. S721–S723, 2011.

[9] A. Widdowson, A. Baron-Wiechec, P. Batistoni, E. Belonohy, J. P. Coad, P. Dinca, D. Flammini, F. Fox, K. Heinola, I. Jepu, J. Likonen, S. Lilley, C. P. Lungu, G. F. Matthews, J. Naish, O. Pompilian, C. Porosnicu, M. Rubel, and R. Villari, "Experience of handling beryllium, tritium and activated components from JET ITER like wall," *Phys. Scr.*, vol. T167, no. 1, p. 014057, 2016.

[10] P. Hovington, D. Drouin, and R. Gauvin, "CASINO: A new monte carlo code in C language for electron beam interaction -part I: Description of the program," *Scanning*, vol. 19, no. 1, pp. 1–14, 2006.

[11] J. Schindelin, I. Arganda-Carreras, E. Frise, V. Kaynig, M. Longair, T. Pietzsch, S. Preibisch, C. Rueden, S. Saalfeld, B. Schmid, J.-Y. Tinevez, D. J. White, V. Hartenstein, K. Eliceiri, P. Tomancak, and A. Cardona, "Fiji: an open-source platform for biological-image analysis," *Nat. Methods*, vol. 9, no. 7, pp. 676–682, Jul. 2012.

[12] C. A. Thompson and L. Andrews, "Reactions of Laser Ablated Be Atoms with H 2 O : Infrared Spectra and Density Functional Calculations of HOBeOH , HBeOH , and HBeOBeH," vol. 1, no. 96, pp. 12214–12221, 1996.

[13] K. Heinola, A. Widdowson, J. Likonen, E. Alves, N. Barradas, S. Brezinsek, N. Catarino, P. Coad, S. Koivuranta, S. Krat, G. F. Matthews, M. Mayer, P. Petersson, and J. E. T. Contributors, "Long-term fuel retention in JET ITER- like wall," *Phys. Scr.*, vol. T167, pp. 1–7, 2016.

[14] A. Widdowson, E. Alves, C. F. Ayres, A. Baron-Wiechec, S. Brezinsek, N. Catarino, J. P. Coad, K. Heinola, J. Likonen, G. F. Matthews, M. Mayer, and M. Rubel, "Material migration patterns and overview of first surface analysis of the JET ITER-like wall," *Phys. Scr.*, vol. T159, no. T159, pp. 1–9, 2014.

[15] M. Kumar[a], C. Makepiece[b], C. Pardanaud[a], Y. Ferro[a], C. Martin[a], P. Roubin[a], A. Widdowson[b], T. Dittmar[c], Ch. Linsmeier[c], C. P. Lungu[d], C. Porosnicu[d], I. Jepu[d], P. Dinca[d], M. Lungu[d], O. G. Pompilian[d], JET Be limiter tiles chemical bonding characterization by means of Raman microscopy and comparison with laboratory Be based samples: Be-O and BeO_xD_y identification in melted region., submitted, (2018).